FEM simulation analysis of wire rod drawing process using the rotating die under Coulomb friction

Gow-Yi Tzou[1], *Un-Chin* Chai[1], *Chao-Ming* Hsu[2,*], and *Hung-Ying* Hsu[2]

[1]Department of Mechanical and Automation Engineering, Chung-Chou University of Science and Technology, Yuanlin, Changhua, 510, Taiwan
[2]Department of Mechanical Engineering, National Kaohsiung University of Applied Sciences, Kaohsiung, 807, Taiwan

Abstract. This study proposes a cold drawing technology of wire rod with rotating die; it carries out an FEM simulation on rotating drawing using DEFORM-3D commercial software. Frictions among the die and the wire material are assumed as Coulomb friction. The effective stress, the effective strain, the velocity field, various stress distributions, the die stress, the drawing force, and the rotating torque can be determined from the FEM simulation. In this study, effects of various drawing conditions such as the rotating angular velocity, the half die angle, the frictional coefficient, the die filet on the drawing forming characteristics are explored effectively. From this FEM simulation, it is noted that the effect of rotation die and die filet can reduce the drawing force and increase the material flow.

1 Introduction

Wire rod drawing process is a high-efficiency and high-precision processing technology, Wire rod is become to the required geometry and dimension after the single pass or multi-passes. Wire rod drawing process has been widely used in various industrial fields, and it is an important indispensable product in industrial countries. Therefore, how to obtaining energy-efficient and rapid production of high-precision wire process technology is actively pursuing at present industries. Kim et al [1] and Yoshida et al. [2] used 3D rigid-plastic finite element method (FEM) to improve the unsteady drawing process of straight-pipe. Lee [3] et al. used the finite element simulation to investigate the manufacturing process of precision linear guide rail through shape rolling and shape Drawing. Haddi et al. [4] studied the temperature increase and tensile stress under different drawing process using a thermocouple and stress sensing system. Zhang et al. [5] explored the temperature increase of wire rod and dies due to the friction at high drawing velocity to calculate the heat of material and friction in the plastic deformation under various lubrications. Due to the high drawing velocity, the material considered the strain rate in flow stress. Tiernan et al. [6, 7] and Huh et al [8] proposed a new load control system of dieless drawing to improve the die wear and lubrication requirements in traditional drawing process. Norasethasopon et al. [9-11] used the finite element simulation to verify the dimensional accuracy and formability of impurities on the drawn copper-containing impurities wire rod. Tiernan et al [12] carried out the experiment of dieless drawing to achieve the ability of reducing wire diameter. Feldera et al [13] proposed the stress analysis due to the friction under temperature of 20 ℃ -150 ℃ in a variety of metal soaps to realize effect of various lubrications to the drawing process. Chen et al [14] used DEFORM-2D with the Taguchi method to design the drawing process of CuZn37 brass alloy considering four control factors such as area reduction, lubrication, drawing velocity and die angle; the optimization of drawing process could be obtained. Based on previous references, traditional drawing process did not consider the die rotation. Tzou et al [15] proposed a cold drawing technology of wire rod with rotating die; it carried out an FEM simulation on rotating drawing using DEFORM-3D commercial software under constant shear friction. The effective stress, the effective strain, the velocity field, and the drawing force have been determined from the FEM simulation. This study assumes the friction to be Coulomb friction different from constant shear friction to explore a cold drawing of wire rod with a rotating die using FEM simulation.

2 FEM simulation

Fig. 1 is a schematic diagram of the drawing process with rotation die. The die is rotated with angular velocity ω (rad/s), the front end of the wire is pulled by the cross head with an initial velocity V_0 (mm/s).

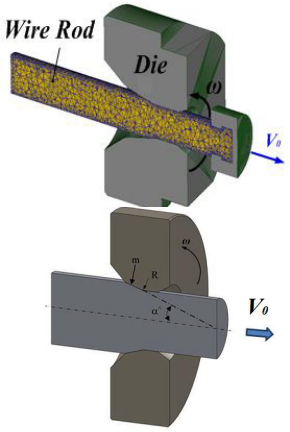

Fig. 1. Schematic diagram of the drawing process with rotation die.

* Corresponding author: jammy@kuas.edu.tw

Table 1 shows FEM simulation parameters of wire rod material in the drawing process with rotating die. The wire rod material is SWRCH22AB (where SWRCH22AB is a carbon steel for Cold Heading and Cold Forging, the chemical composition: C=0.18-0.23%, Si=0.1%, Mn=0.7%-1.0%, P=0.03%, S=0.035%; the Young's modulus 210GPa and Poisson's ratio 0.3. The flow stress shown in Fig. 2 can be obtained by the compress test, $\sigma = 832.233\ \varepsilon\ 0.382$. The initial diameter (Do) is 6.4mm; the number of mesh element is 60,000; the drawing velocity is 33.50mm/s. Table 2 shows FEM simulation parameters of dies in the drawing process with rotation die. The die diameter (Dd) is 5.6mm; the rotating angular velocity (ω) is set to 0~4.5 rad/s; the half die angle (α) is set to 10 ° ~ 18 °; the Coulomb frictional coefficient (μ) is assumes as 0.05, 0.1, and 0.15, respectively, and the die filet (R) is 3 ~ 7mm.

Table 1. FEM simulation parameters of wire rod material in the drawing process with rotation die.

Wire Rod Conditions	
Material	SWRCH22AB
Wire Diameter D_o (mm)	6.4
Wire Velocity V_0 (mm/s)	33.50
Elements	60000

Table 2. FEM simulation parameters of dies in the drawing process with rotation die.

Die Conditions	
Die Diameter D_d (mm)	5.6
Half Die Angle α (°)	10°,14°,18°
Frictional Coefficient μ	0.05, 0.1, 0.15
Die Filet R (mm)	3, 5, 7
Rotating Angular Velocity ω (rad/s)	0.5, 2.5, 6.5

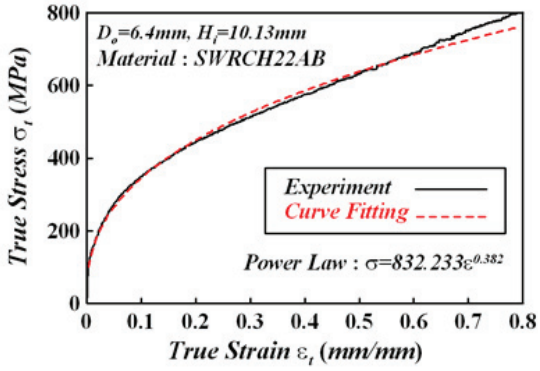

Fig. 2. Flow stress for SWRCH22AB wire rod in compression test.

Because considering the rotation effect, the Deform 2D software cannot be used, therefore in the study the Deform 3D software should be used in the drawing process with rotation die.

3 Results and Discussions

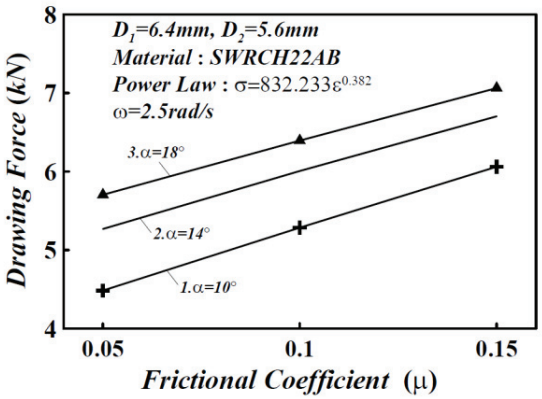

Fig. 3. Variations of drawing force with frictional coefficient for various half die angles.

Fig. 3 shows variations of drawing force with frictional coefficient for various half die angles. The drawing force is increased with an increase of the frictional coefficient under the fixed half die angle. Under the fixed frictional coefficient, the drawing force is increased with an increase of half die angle.

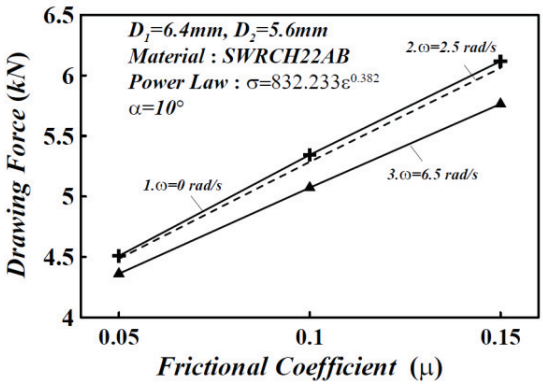

Fig. 4. Variations of drawing force with frictional coefficient for various angular velocities.

Fig. 4 shows variations of drawing force with frictional coefficient for various angular velocities. The drawing force is reduced with an increase of rotating angular velocities. As the rotating angular velocity increases to make the hoop frictional stress increased.

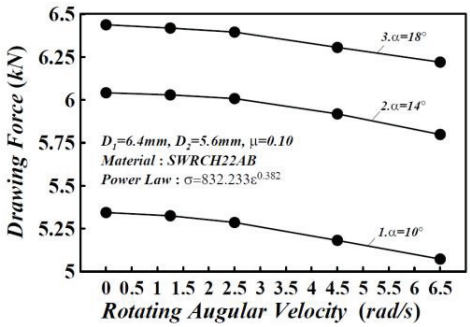

Fig. 5. Variations of drawing force with rotating angular velocity for various half die angles.

Fig. 5 shows variations of drawing force with rotating angular velocity for various half die angles. It reveals that the drawing force is reduced as the rotating angular velocity increases**.**

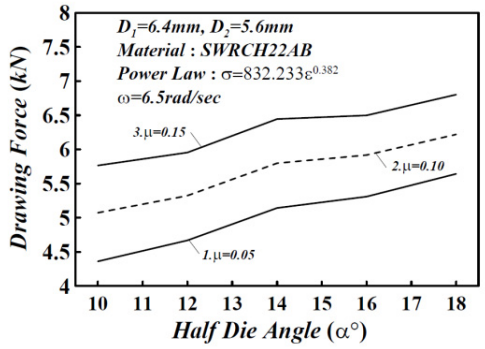

Fig. 6. Variations of drawing force with half die angles for various frictional coefficients.

Fig. 6 shows variations of drawing force with half die angles for various frictional coefficients. As the half die angle increases the drawing force increases under the fixed frictional coefficient.

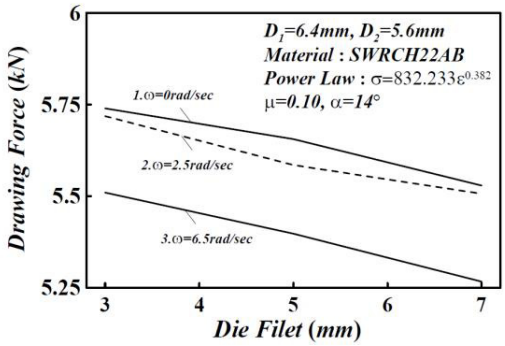

Fig. 7. Variations of drawing force with die filets for various angular velocities.

Fig. 7 shows variations of drawing force with die filets for various angular velocities. The drawing force is reduced with an increase of die filet. As the die filet increases the material is easy to deform.

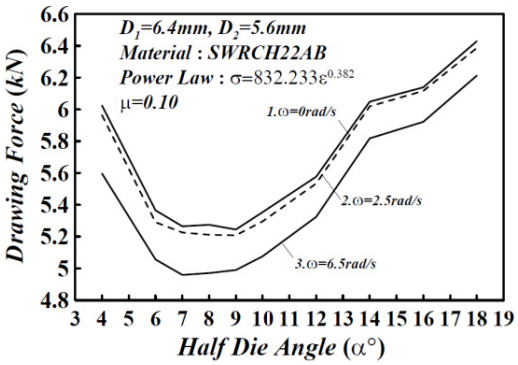

Fig. 8. Variations of drawing force with half die angle for various angular velocities.

With a view to realizing what the optimum half die angle under different rotating angular velocities is. Fig. 8 shows the optimum half die angle decreases with an increase of rotating angular velocity. As the half die angle does not exceed the optimum half die angle, the drawing force is reduced due to a decrease of frictional stress along the interface between die and material. However, as the half die angle exceeds the optimum half die angle, the material deformation effect is larger than the frictional stress effect so that the drawing force is increased.

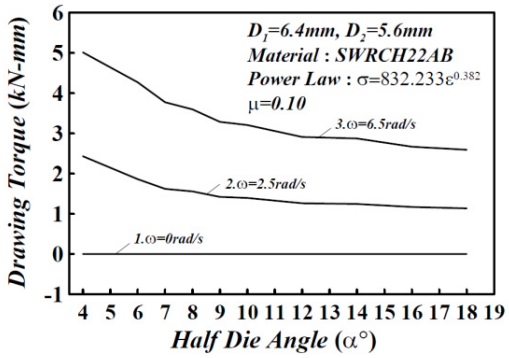

Fig. 9. Variations of drawing torque with half die angle for various angular velocities.

Fig. 9 shows variations of drawing torque with half die angle for various angular velocities. Without the die rotation, no drawing torque is occurred. The rotating angular velocity increases to make the drawing torque increased. Under the fixed angular velocity, the drawing torque is reduced with the increase of half die angle.

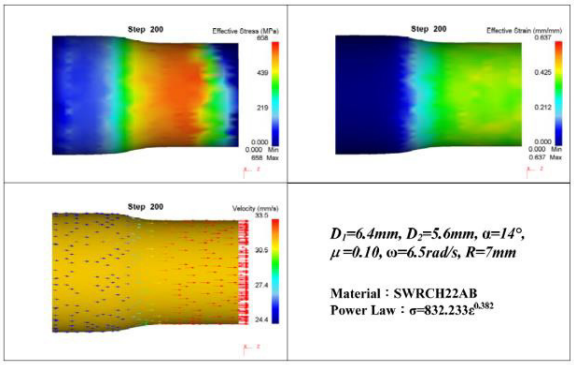

Fig. 10. Effective stress, effective strain, and velocity field with the rotating die.

Fig. 10 shows effective stress, effective strain, and velocity field with the rotating die. Under these conditions, the maximum effective stress is 658MPa; the maximum strain is 0.637 mm/mm; the maximum flow velocity is 33.5 mm/s; the drawing force is 5.799 kN.

4 Conclusions

This study uses FEM simulations to obtain the effective stress, the effective strain, the velocity field, drawing force, and drawing torque. The major results can be summarized as follows:

1. Optimum half die angle can be obtained from FEM simulation, and it is decreased with an increase of rotating angular velocity.

2. Drawing torque is changed with the frictional stress along the interface between die and material.

3. After the optimum half die angle, as the half die angle (α) increases, the internal plastic deformation is more intense so that the drawing force increases.

4. As the frictional coefficient (μ) increases, the frictional resistance is large so that the drawing force increases.

5. As the die filet (R) increases, the material flow is smoother so that the drawing force decreases.

6. As the rotating angular velocity (ω) increases, the material flow is smoother so that the drawing force decreases.

Acknowledgments

Thanks for MOST project's financial supports (MOST 104-2221-E-235-002) to complete this research.

References

1. H. C. Kim, Y. Choi, B. M. Kim, Three-Dimensional Rigid-Plastic Finite Element Analysis of Non-Steady-State Shaped Drawing Process, *International Journal of Machine Tool and Manufacture*, **39** (1999) 1135-1155

2. K. Yoshida, H. Furuya, Mandrel Drawing and Plug Drawing of Shape-Memory-Alloy Fine Tubes Used in Catheters and Stents, *Journal of Materials Processing Technology*,**153-154** (2004) 145-150

3. S. H. Lee, S. K. Lee, B. M. Kim, Study on The Manufacturing Process of Precision Linear Guide Rail Through Shape Rolling and Shape Drawing, *Journal of Mechanical Science and Technology*, **24** (2010) 1647-1653

4. A. Haddi, A. Imad, G. Vega, Analysis of Temperature and Speed Effects on the Drawing Stress for Improving the Wire Drawing Process, *Materials and Design*, **32** (2011) 4310-4315

5. J. Zhang, J. Sun, J. Long, S. Tang, Computer Simulation on Temperature Rise in Process of Wire Drawing, *Journal of Shanghai Jiaotong University*,**E-5** (2000) 242-247

6. P. Tiernan, R. Carolan, E. Twohig, S. A. M. Tofail, Design and Development of A Novel Load-Control Dieless Rod Drawing System, *CIRP Journal of Manufacturing Science and Technology*, **4** (2011) 110-117

7. P. Tiernan, M. T. Hillery, Dieless Wire Drawing-An Experimental And Numerical Analysis, *Journal of Materials Processing Technology*,**155-156** (2004) 1178-1183

8. Y. Huh, B. K. Ha, J. S. Kim, Dieless Drawing Steel Wires Using A Dielectric Heating Method and Modeling the Process Dynamics, *Journal of Materials Processing Technology*, **210** (2010) 1702-1708

9. S. Norasethasopon, H. Yoshida, Finite Element Simulation of Inclusion Size Effects on Copper Shape-Wire Drawing, *Materials Science and Engineering*, **422** (2006) 252-258

10. S. Norasethasopon, H. Yoshida, Influences of Inclusion Shape and Size in Drawing of Copper Shaped-Wire, *Journal of Materials Processing Technology*, **172** (2006) 400-406

11. S. Norasethasopon, K. Yashida, Prediction of Chevron Crack Initiation in Inclusion Copper Shaped-Wire Drawing, *Engineering Failure Analysis*,**15** (2008) 378-393

12. P. Tiernan, M. T. Hillery, An Analysis of Wire Manufacture Using the Dieless Drawing Method, *Journal of Manufacturing Processes*,**10** (2008) 12-20

13. E. Feldera, C. Levraua, M. Mantel, N. G. T. Dinh, Identification of the Work of Plastic Deformation and the Friction Shear Stress in Wire Drawing, *Wear*, **286-287** (2012) 27-34

14. D. C. Chen, J. Y. Huang, Design of Brass Alloy Drawing Process Using Taguchi Method, *Materials Science and Engineering*,**464** (2007) 135-140

15. G. Y. Tzou, D. C. Chen, S. H. Lin, Study on Wire Rod Drawing Process using the Rotating Die, *Key Engineering Materials*,**76** (2016) 63-67